NIH Public Access
Author Manuscript
Int J Radiat Oncol Biol Phys. Author manuscript; available in PMC 2009 June 13.

Published in final edited form as:
Int J Radiat Oncol Biol Phys. 2007 October 1; 69(2): 444–453. doi:10.1016/j.ijrobp.2007.03.018.

Radiotherapy treatment of early stage prostate cancer with IMRT and protons: a treatment planning comparison

Alexei Trofimov, Ph.D., **Paul L. Nguyen, M.D.**, **John J. Coen, M.D.**, **Karen P. Doppke, M.S.**, **Robert J. Schneider, C.M.D.**, **Judith A. Adams, C.M.D.**, **Thomas R. Bortfeld, Ph.D.**, **Anthony L. Zietman, M.D.**, **Thomas F. DeLaney, M.D.**, and **William U. Shipley, M.D.**
Department of Radiation Oncology, Massachusetts General Hospital and Harvard Medical School, Boston, MA, 02114 USA

Abstract

Purpose—To compare intensity-modulated photon radiotherapy (IMRT) with 3D-conformal proton therapy (3D-CPT) for early stage prostate cancer, and explore the potential utility of intensity-modulated proton therapy (IMPT).

Methods—Ten patients were planned with both 3D-CPT (2 parallel-opposed lateral fields) and IMRT (7 equally spaced coplanar fields). Prescribed dose was 79.2 Gy (or cobalt Gray-equivalent, CGE for protons) to the prostate gland. Dose-volume histograms, dose conformity, and equivalent uniform dose (EUD) were compared. Additionally, plans were optimized for 3D-CPT with non-standard beam configuration, and for IMPT assuming delivery with beam scanning.

Results—At least 98% of the PTV received the prescription dose. IMRT plans yielded better dose conformity to the target, while proton plans achieved higher dose homogeneity, and better sparing of rectum and bladder in the range below 30 Gy/CGE. Bladder volumes receiving over 70 Gy/CGE (V_{70}) were reduced, on average, by 34% with IMRT vs. 3D-CPT, while rectal V_{70} were equivalent. EUD from 3D-CPT and IMRT plans were indistinguishable within uncertainties, for both bladder and rectum. With the use of small-angle lateral-oblique fields in 3D-CPT and IMPT, the rectal V_{70} was reduced by up to 35% compared to the standard lateral configuration, while the bladder V_{70} increased by less than 10%.

Conclusions—In the range over 60 Gy/CGE, IMRT achieved significantly better sparing of the bladder, while rectal sparing was similar with 3D-CPT and IMRT. Dose to healthy tissues in the range below 50% of the target prescription was substantially lower with proton therapy.

Keywords

prostate cancer; comparative treatment planning; intensity-modulated radiotherapy (IMRT); 3D-conformal proton therapy; intensity-modulated proton therapy (IMPT)

Corresponding author: Alexei Trofimov, Ph.D. Mailing address: Department of Radiation Oncology, Massachusetts General Hospital, 30 Fruit Street, Boston, MA 02114, Telephone: (617) 724-3655, Fax: (617) 714-0368, E-mail: E-mail: atrofimov@partners.org.

Conflict of Interest Notification: The authors declare NO conflict of interest in relation to this manuscript.

Publisher's Disclaimer: This is a PDF file of an unedited manuscript that has been accepted for publication. As a service to our customers we are providing this early version of the manuscript. The manuscript will undergo copyediting, typesetting, and review of the resulting proof before it is published in its final citable form. Please note that during the production process errors may be discovered which could affect the content, and all legal disclaimers that apply to the journal pertain.

NIH-PA Author Manuscript
NIH-PA Author Manuscript
NIH-PA Author Manuscript

NIH-PA Author Manuscript

NIH-PA Author Manuscript

NIH-PA Author Manuscript

INTRODUCTION

Conformal proton therapy was first delivered to prostate cancer patients in 1976 at the Harvard Cyclotron, with the clinical support from Massachusetts General Hospital (MGH). As the proton dose is largely deposited in the Bragg peak at the end of the particle's range, with no dose delivered beyond a few millimeters past the peak, protons offer a great tool for sparing of the healthy tissue around the target. The method currently employed at the MGH Francis H. Burr Proton Therapy Center is 3D-conformal proton therapy (3D-CPT) using broad passively-scattered proton beam (1). Patient-specific devices are used to shape the radiation field: brass apertures for lateral, and lucite compensators for distal conformation. Uniform target coverage in depth is achieved by modulating the energy of the proton beam entering the patient's body, to create a spread-out Bragg peak.

Since the first publication from 1979, based on 17 cases treated at MGH (2), clinical experience with protons in prostate cancer has grown greatly. In 1995, MGH reported on a Phase III randomized trial of high dose irradiation boosting with conformal protons to a dose of 75.6 cobalt Gray-equivalent (CGE), compared with conventional irradiation to 67.2 Gy using photons alone for patients with stage T3–T4 disease (3). Loma Linda Proton Treatment Center published their initial experience with 1277 patients with early disease, treated to 74 CGE, and found comparable disease-free survival with minimal morbidity, compared to other forms of local therapy (4). Recently, a randomized two-arm dose-escalation trial that involved a mix of photons and protons to treat localized prostate cancer at MGH and Loma Linda, found that irradiation to 79.2 vs. 70.2 CGE produced a significantly superior 5-year PSA-failure-free survival (5).

As protons are still a rather limited resource, it is important to identify the sites in which proton therapy offers appreciable advantage over the more readily available conformal treatments, such as intensity-modulated radiotherapy (IMRT) with photons.

Patients with early prostate cancer were among the first to benefit from the clinical use of IMRT in the mid-1990s (6). By employing advanced inverse treatment planning techniques, IMRT allowed for improvement in the dose distribution conformity to the tumor volume, and, consequently, a reduction in irradiation of the healthy surrounding tissue. While the dosimetric advantage of IMRT over the standard 3D-conformal photon therapy has been widely reported (7–11), a comprehensive planning comparison of IMRT and proton radiation therapy has not been performed thus far.

Cella *et al.* compared 3D-conformal and intensity-modulated proton and photon plans for a single case of prostate cancer (12); and Mock *et al.* compared 3D-conformal photon and proton plans with photon IMRT for 5 patients (13). However, the proton range uncertainty was not taken into account in the design of treatment plans.

The primary purpose of this study was to determine the relative dosimetric benefits and disadvantages of IMRT vs. 3D-conformal proton therapy for patients with prostate cancer, taking into account proton range uncertainty. Secondly, we investigated the utility, for prostate cancer, of intensity-modulated proton therapy (IMPT).

Similar to IMRT with photons, IMPT delivers individually inhomogeneous dose distributions from various directions to yield the desired distribution. IMPT can be delivered by magnetically scanning a narrow proton beam across the target volume. Beam intensity and speed are varied during the scan to achieve the desired dose modulation, and the beam energy is adjusted for irradiation of specific layers of equal radiological depth within the target. In this way, IMPT makes it possible to conform the dose to the proximal edge of the target, in addition to the distal edge (as in 3D-CPT). Unlike 3D-CPT, IMPT does not require patient-specific range

NIH-PA Author Manuscript

NIH-PA Author Manuscript

NIH-PA Author Manuscript

compensators. Consequently, IMPT avoids the additional proton beam scattering in the compensator material, upstream from the patient, and reduces the degradation of the dose penumbra in tissue. IMPT treatments have not yet been delivered in the United States. Work on the implementation of clinical IMPT is currently under way at MGH.

The experience with IMPT at Paul Scherrer Institut (Switzerland) demonstrated a potential for improved tissue sparing in a number of sites, including intracranial, nasopharyngeal and paraspinal lesions (14–18). While intensity-modulation has been identified as a means to achieve prostate dose escalation (12), IMPT treatment of prostate cancer has not yet been performed anywhere.

METHODS

Patient selection

After approval by the MGH Investigational Review Board for this treatment planning comparison study, we randomly selected ten patients with clinically localized early stage prostate cancer, who were treated with protons. Among patients who require radiation treatment to the prostate and seminal vesicles only (i.e., not the pelvic nodes), the choice between IMRT and proton therapy at MGH is most commonly based on the treatment slot availability and patient preferences, rather than any clinical characteristics.

Treatment simulation

CT scanning was performed in the supine position with the resolution between 0.93 and 0.98 mm in the axial planes, and the slice thickness of 2.5 mm. The attending physician outlined the entire prostate, the most caudal 1-cm section of the seminal vesicles, the entire rectal wall from the junction with the sigmoid colon to the anus, urinary bladder, penile bulb, and femoral heads.

For each patient, the gross tumor volume (GTV) was considered the prostate gland, and the clinical target volume (CTV) was defined as the whole prostate and caudal seminal vesicles. Two planning volumes, PTV1 and PTV2 were defined as 5-mm uniform expansions around CTV and GTV, respectively. Dose prescriptions were applied as recommended in RTOG protocol 0126 (Table 1). The CTV prescription dose was 50.4 Gy or CGE (for protons), and the GTV prescription was 79.2 Gy/CGE. For conversion to cobalt Gray-equivalent, the physical dose was multiplied by the radiobiological effectiveness (RBE) of the proton, which was assumed to be 1.1 relative to Co-60.

The average GTV volume was 67 cc (30 cc minimum, 120 cc maximum, 56 cc median). The sizes of target volumes for all patients are given in Table 2.

Treatment planning

Clinical 3D-conformal proton therapy plans were created with CMS/XiO software (CMS Inc., St.Louis, Missouri). Two equally weighted parallel-opposed lateral fields were used to deliver the prescribed dose to the CTV, and the boost dose to the GTV. The dose was calculated on a $2\times2\times2.5\ mm^3$ grid.

While the sharp dose fall-off beyond the proton Bragg peak presents a valuable tool for tissue sparing, precise positioning of the distal dose gradient is complicated by the uncertainties in the proton penetration depth. In a fractionated treatment course, radiological path length for the incoming proton beam may vary day-to-day due to misalignment of tissue inhomogeneities, especially bony structures, and the compensator, as the result of variation in the patient positioning (19). To ensure adequate PTV coverage despite the uncertainties in alignment with

NIH-PA Author Manuscript

NIH-PA Author Manuscript

NIH-PA Author Manuscript

bony structures that will be introduced by shifts made as part of the daily image-based patient set-up, a technique called “compensator smearing” is employed at the MGH proton center. An idealized range compensator is first designed by the treatment planning system based on the planning CT data. The compensator map consists of hexagonal elements, of 3 mm in diameter (Figure 1). Each element is assigned the thickness of material needed to stop the protons at the distal surface of the target volume. Typically, the 98% isodose is matched to the planning target outline (1). The “smear” algorithm is then applied, in which each of the hexagonal elements is reassigned the thickness to the value, that is the lowest among its nearest neighbors within the given “smear radius”. This procedure ensures that misalignments within the smear radius will not compromise the dose coverage of the PTV. However, consequently, the prescription isodose surface is pushed beyond the PTV surface and, inevitably, the dose to healthy tissue distally to the target is increased. Prostate treatment plans typically employ the smear radius of 10 mm.

A clinical physicist used Corvus treatment planning software (NOMOS corp., Sewickley, PA) to create the photon IMRT plans. All plans employed 7 coplanar beams of 6 MV, spaced by 50° from the posterior direction. The plans were optimized for delivery with a MLC of 5×5 mm^2 resolution at the isocenter.

Since, beyond a narrow build-up region close to the skin surface, the photon dose falls off exponentially with depth, the consequence of errors associated with tissue inhomogeneities is typically not as grave as in the case of the protons. However, the inter-fractional motion of prostate, bones of the hip, and other changes related to rectal or bladder filling may significantly affect the conformity of treatment (20). In the presence of position uncertainties, PTV margins ensure the target coverage with IMRT.

To explore the potential for treatment improvement, a number of experimental proton plans were optimized for selected patients. These included 3D-CPT plans in which dose was delivered from anterior-oblique direction, and IMPT plans optimized for delivery with proton pencil beam scanning.

Unlike the clinical plans that used parallel-opposed lateral beams (gantry angles of 90° and 270°), experimental 3D-CPT plans were optimized with the beams rotated towards the anterior direction (e.g., for a 20° anterior rotation, to 70° and 290°). This allowed for taking advantage of the sharp distal penumbra of the proton beam. At the typical depth of target in prostate treatments (20–30 cm water-equivalent), the lateral penumbra of the proton beam deteriorates substantially due to Coulomb scattering, and becomes roughly twice as wide as the distal penumbra. However, in the current clinical practice, the use of distal gradients for dose conformation is avoided, due to the uncertainty in the proton penetration depth.

Treatment plans for IMPT were created with KonRad Pro software, developed at German Cancer Research Center (DKFZ). KonRad employs inverse planning methods to optimize relative weights of individual pencil beams, to achieve the desired dose coverage (21–23). IMPT plans used lateral parallel-opposed beam configuration, and were optimized for delivery with a pencil beam of σ=5 mm (approximately 12 mm full width at half-maximum, as projected for the MGH proton scanning nozzle).

Planning margins, identical to those in respective IMRT plans, were used to ensure the target coverage with IMPT. Since IMPT dose is modulated in 3 dimensions (laterally and in depth), dose homogeneity may be affected by misestimating the proton radiation depth. To ensure the dose uniformity and its conformity to the target, real-time monitoring of IMPT delivery may be needed, e.g., using positron emission tomography (24,25).

NIH-PA Author Manuscript

NIH-PA Author Manuscript

NIH-PA Author Manuscript

Treatment delivery

At MGH, prostate patients are treated in supine position. Immobilization is achieved with commercially available rigid devices, such as the leg abductor (Alimed Inc., Dedham, MA). Daily pre-treatment imaging with a B-mode Acquisition and Targeting ultrasound probe (NOMOS corp., Sewickley, PA) is used to align the target with the treatment field, for both IMRT and 3D-CPT. Except for hip rotation, set-up is identical for IMRT and proton therapy.

Application of smear algorithm in the proton compensator design ensures that the effect of the set-up uncertainties on the radiological path length to the target does not compromise the target dose coverage. Portal X-ray imaging is performed daily during the first week of treatment, to ensure correct positioning of the range compensator with respect to the bony anatomy and the prostate (26). If the alignment of bony anatomy from portal imaging and prostate from ultrasound is consistently within the 5-mm agreement, X-ray imaging is performed weekly for the rest of the course (while target localization and alignment using the ultrasound probe are still done daily for all patients). In fewer than 5% of prostate treatment courses, in which the default smear radius of 10 mm is judged insufficient, a new compensator is manufactured with increased smear.

All ten subjects of this study were treated with 3D-conformal proton therapy. Two lateral fields were used to deliver the prescription dose to the CTV in 25 fractions, followed by the 16-fraction dose boost to the GTV.

Endpoints

Dose-volume histograms (DVH) were calculated for all volumes of interest. The DVH parameters used in the comparison of IMRT and proton plans included the minimum, mean, maximum doses, for targets; $D_{35\%}$ (i.e., the dose exceeded in 35% of the given volume), $D_{25\%}$, $D_{15\%}$, and $D_{2\%}$ for healthy organs. Also compared were the fractional volumes that received a certain dose, e.g., V_{60} (the fraction of the volume of interest that received at least 60 Gy/CGE), V_{70}, etc. The Wilcoxon matched-pair signed-rank test was applied to evaluate the level of significance of the observed difference between dose-volume metrics. The threshold of statistical significance was set at $p \leq 0.05$.

Equivalent uniform doses (EUD) were evaluated as $EUD = \left[\frac{1}{N} \sum_{i}^{N} (d_i)^{\alpha} \right]^{1/\alpha}$, where α is a tissue-specific parameter, and N is the total number of points (voxels) i in the volume of interest for which the physical dose d_i was calculated (27,28). The parameter α is typically positive for healthy organs and negative for target volumes. The values of α were kindly provided by A. Niemierko, Ph.D. (MGH). The EUD for target volumes were calculated with $\alpha = -10^{+3}_{-5}$, where the subscript and superscript designate the uncertainty margins (95% confidence). EUD were evaluated for the central (most probable) value of α, as well as the uncertainty bounds: e.g., for a target, α =−10 (central value), −15 (lower bound) and −7 (upper bound). The values of α for healthy organs were as follows: $\alpha = 7^{+5}_{-3}$ for the bladder, $\alpha = 5^{+3}_{-2}$ for the rectum.

The dose conformity index was calculated as the ratio of the prescription isodose volume to the volume of the corresponding target. If target coverage is equivalent for two plans, the one with better dose conformity will have a smaller conformity index. Ideally, conformity index would be 1, if the prescription isodose coincides with the target surface.

NIH-PA Author Manuscript

NIH-PA Author Manuscript

NIH-PA Author Manuscript

RESULTS

Dose delivery to target

Plan objectives with respect to the target coverage were fulfilled in all cases: at least 98% of PTV2 received 79.2 Gy/CGE. Minimum, mean and maximum GTV and CTV doses are given in Table 3. Sample 3D-CPT and IMRT dose distributions in the transversal isocenter plane are shown in Figures 2 (Patient 1) and 4 (Patient 2), and corresponding DVH are plotted in Figures 3 and 5, respectively.

IMRT dose distributions proved more conformal to the target, with the volume of the 79.2-Gy isodose reduced, on average, by 26% (p=0.002), compared to 3D-CPT plans (see Table 2). For PTV1, the average conformity index was 2.73 with IMRT vs. 3.11 in 3D-CPT plans (p=0.004). As illustrated in Figure 6, IMRT irradiated substantially greater volumes of tissue in the low dose range (below 30 Gy), while 3D-CPT irradiated roughly 20% larger volumes in the medium-to-high range (50–75 Gy).

Dose homogeneity within the GTV was higher with protons. In 3D-CPT plans, the difference between minimum and maximum GTV doses was on average only 3.7 CGE (see Table 3). IMRT plans delivered hot spots of up to 115% of the prescription dose, with between 1 and 3% of the GTV receiving in excess of 110% of the prescription dose (≥87.1 Gy). While the extent of dose inhomogeneity in IMRT is, somewhat, influenced by the algorithm (planning software), generally, hot spots arise in inverse plan optimization from the placement of sharp dose gradients at the interface between the target and healthy tissue. A reduction in the hot volume may be achieved at the price of decreased dose conformity.

Incidental dose to surrounding normal tissues

The difference between the IMRT and 3D-CPT dose distributions for Patient 2 is shown in Figure 4c. The protons delivered excess dose to the volume immediately surrounding the target (due to the broader penumbra and the effect of compensator smear), and laterally, along the direction of irradiation. Elsewhere, IMRT irradiated healthy tissues to higher doses.

Dose-volume metrics for the rectum and bladder, along with the results of comparison using the Wilcoxon test, are summarized in Table 4. The excess dose that protons delivered in the region surrounding the target led to a 10%-increase in $D_{15\%}$ to the bladder, compared to IMRT (p=0.006). The fraction of the bladder volume irradiated to 60 Gy/CGE (V_{60}) was on average 30% higher, while V_{70} was over 50% higher with 3D-CPT (p=0.002). The difference, between IMRT and proton plans, in rectal V_{70} was not statistically significant. Mean doses were reduced with protons vs. IMRT, by 26% in the rectum (p=0.002) and by 20% in the bladder (p=0.006). In the lower dose range, the rectal V_{30} was reduced with protons vs. IMRT by between 16% (in Patient 8) and 53% (Patient 2). Neither IMRT nor 3D-CPT demonstrated a clear advantage based on other dose-volume metrics (e.g., V_{60}, $D_{35\%}$ for rectum, $D_{25\%}$ for both rectum and bladder).

Bladder and rectum DVH for all patients are shown in Figure 7. No correlation was observed between the target size and doses to these organs. In all plans, the doses to femoral heads and penile bulb were well below the tolerances recommended by RTOG protocol 0126 (see, e.g., Figures 3, 5).

Comparison using equivalent uniform dose

Equivalent uniform doses are summarized in Table 5. Due to the relatively high target dose homogeneity, the assumed uncertainties in the value of the EUD parameter α translated into negligible uncertainties in the GTV EUD (0.04 Gy on average for IMRT, 0.02 CGE for 3D-

NIH-PA Author Manuscript

NIH-PA Author Manuscript

NIH-PA Author Manuscript

CPT). The EUD differed from the mean GTV dose by less than 0.1 Gy/CGE, in either IMRT or proton plans. In the bladder and rectum, the difference between the proton and IMRT EUD was insignificant, given the uncertainties in the value of α.

3D-conformal proton therapy plans with non-standard beam configuration

The use of anterior oblique beams in experimental 3D-CPT plans allowed for a reduction in the dose to rectum, as the advantage was taken of placing the sharp distal dose fall-off in front of the rectal volume (see Figures 4d, 5). Additionally, as the amount of bony tissue in the beam path was reduced, compared to the lateral parallel-opposed beam configuration, the lateral penumbra also improved due to reduced scattering. For Patient 2, with the 20° beam rotation towards the anterior (Figure 4d), the rectal V_{70} was reduced by 35%, while the bladder V_{70} increased by less than 10%. The increase in the bladder dose, however, became rather substantial in plans that used larger anterior oblique angles. With the beams rotated to 50° from the lateral direction, the bladder V_{70} increased by a factor of 2.5, compared to the plan using the parallel-opposed lateral configuration, while the gain in rectal sparing was comparable to that achieved with the 20° rotation. A potential problem with the use of anterior oblique beams is the increased uncertainty in proton penetration depth due to the intra-fractional variation in the filling of the bladder.

IMPT plans

With IMPT, it was possible to reduce the dose to the rectum and bladder, compared to 3D-CPT, both for the parallel-opposed and small-angle anterior oblique beam configurations. A sample IMPT dose distribution is shown in Figure 2c, and the corresponding DVH in Figure 3. For the case illustrated in Figure 2c, PTV1 conformity index was 1.65, improved by 35% compared to the IMRT plan. Figure 8 shows the IMPT dose distributions delivered by each of the two parallel-opposed beams. While the dose delivered by each beam in 3D-CPT is approximately uniform throughout the target, IMPT beams delivered higher dose to the respective “proximal” parts of the target. Thus, IMPT took advantage of better penumbra characteristics of the lower energy beams.

DISCUSSION

Massachusetts General Hospital is one of only a few sites worldwide that operate both IMRT and particle therapy facilities. Therefore, this study was able to draw on the unique first-hand experience in clinical treatment planning and therapy of prostate cancer. Previously, Cella *et al.* reported on the comparison of 3D-conformal and intensity-modulated proton and photon plans for a single case (12). The plans were designed with rather relaxed target coverage, with the prescription dose of 81 Gy delivered to roughly 50% of the PTV. Intensity-modulation (with either photons or protons, using the same 5-field configuration) improved target dose homogeneity, reduced normal tissue irradiation in the low and medium range (≤70% of the target dose), and allowed for escalation of the median target dose from 81 to 99 Gy. More recently, Mock *et al.* compared treatment plans for 3D-CPT and photon IMRT for 5 patients, using the prescription dose of 70 Gy (13). The difference in the rectum and bladder volumes that received 70% of the prescription dose was found to be insignificant, while the mean doses to healthy organs were reduced by between 40% and 80% with protons.

The plans presented in this manuscript used the target volume definitions and dose prescriptions recommended by RTOG protocol 0126. The 3D-conformal proton therapy plans were optimized for actual treatment courses delivered at MGH, and used standard strategies to minimize the effect of the delivery uncertainties. The reduction, with 3D-CPT vs. IMRT, of the mean dose to rectum (by 26%, on average) and bladder (by 20%) was not as significant as previously reported (12,13). While IMRT achieved significant improvement in bladder sparing

NIH-PA Author Manuscript

NIH-PA Author Manuscript

NIH-PA Author Manuscript

(e.g., V_{60}, V_{70}), neither appeared to have a clear advantage in rectal sparing in the high-dose range (over 70% of the GTV prescription).

In radiation treatment of prostate cancer, there is no single accepted predictive factor based on the dose to healthy tissue, which is correlated with treatment complications. Various clinical indications for the development of late rectal toxicity have been reported: e.g., irradiation of 40% of the whole rectal volume to 65 Gy (29), 25% to 66 Gy (30), 57% to 60 Gy (31), or $D_{25\%}$ of 70 Gy (32). Based on the data from randomized trials at MGH, Benk *et al*. advised caution in raising more than 40% of the anterior rectal wall (or, roughly, 20% of the whole rectum) to 75 CGE (33), while Hartford *et al*. linked increased risk of rectal toxicity to irradiation of over 70% of the anterior wall to 60 Gy, and over 30% to 75 Gy (34).

Among the cases examined in this study, Patient 5, who received 70 CGE to 26.5%, and 75 CGE to 21.3% of the whole rectal volume, according to the clinical 3D-CPT plan, indeed suffered from acute rectal toxicity. Incidentally, in the respective IMRT plan, only 16.6% of the rectal volume received 70 Gy or more, a reduction of almost 40% from the proton plan. For the same patient, V_{75} was smaller by nearly a factor of 2 with IMRT (11.0% vs. 21.3% with protons). In the other nine cases, for either 3D-CPT or IMRT, rectal V_{70} and V_{75} were all safely below the abovementioned risk-indicating levels. This result indicates that, due to their capacity for creating sharp dose gradients, intensity-modulated treatments (with photons or protons) are likely to decrease the odds of acute complications in prostate cancer patients in certain problematic anatomical configurations. In less challenging circumstances, the potential of intensity-modulation may not necessarily be engaged in full to achieve acceptable levels of organ sparing. Consequently, IMRT may be more suitable in cases where such complications appear likely, e.g. judging by the DVH metrics of 3D-conformal plans.

While, in terms of EUD, or in the physical dose range of 50 to 70 Gy, there appeared to be no significant difference in sparing of healthy tissue with either protons or IMRT, the protons irradiated substantially smaller volumes in the range up to 30 Gy. As more than 70% of all prostate cancers in the U.S. are diagnosed in males over age 65, the benefit of the integral dose reduction with protons may not be as appreciable as in younger age groups. However, recent reports of the increased risk of secondary malignancies in the older population, following prostate cancer radiotherapy (35–37), indicate that the dose reduction may be practical in that demographic group as well.

Concerns have been raised about the effect of the whole-body dose from neutrons produced in proton interactions with, e.g., the beam-shaping devices during 3D-CPT treatments (38–40). Notably, the compact (often referred to as “spherical”) shape of the target in prostate treatments allows for design of apertures, which are more material-efficient compared to those needed for targets having more complicated shapes. Thus, the amount of material in the beam path and, consequently, the dose from secondary particles are reduced. In the case of prostate treatment, roughly equal numbers of secondary neutrons are produced in proton interactions with the aperture material (externally), and the patient tissue (internally). Intensity-modulated proton therapy with a scanned pencil beam, IMPT may completely avoid the use of field-shaping apertures, and further reduce the dose from secondary particles.

IMPT is routinely delivered to cancer patients at PSI (Switzerland) (14,16,18). The work on development and clinical implementation of IMPT is currently under way at MGH and other proton centers in the US and internationally. While beam scanning may initially be a more time-consuming and costly alternative to the established passive-scattering proton therapy, the differential is expected to abate as IMPT becomes a more common treatment option.

The uncertainty in the particle penetration depth is the main factor that limits sparing of healthy tissue with proton therapy. Currently, standard proton treatments of prostate cancer employ

NIH-PA Author Manuscript

NIH-PA Author Manuscript

NIH-PA Author Manuscript

parallel-opposed lateral beams, which are considered least affected by the proton range uncertainty. However, lateral approach is also associated with the largest radiological depth of the target, thus, higher scatter and wider dose penumbra. With improved range verification, proton dose conformity would improve substantially, especially with the possibility, offered by IMPT, to conform to the target proximally. The improved dose conformity to the target, in turn, will make feasible the target dose escalation while maintaining adequate sparing of healthy organs.

Acknowledgments

This work was supported in part by the NCI program project grant 5P01-CA21239-25 “Proton radiation therapy research”.

References

1. Bussiere MR, Adams JA. Treatment planning for conformal proton radiation therapy. Technol Cancer Res Treat 2003;2:389–399. [PubMed: 14529304]
2. Shipley WU, Tepper JE, Prout GR Jr, et al. Proton radiation as boost therapy for localized prostatic carcinoma. JAMA 1979;241:1912–1915. [PubMed: 107338]
3. Shipley WU, Verhey LJ, Munzenrider JE, et al. Advanced prostate cancer: the results of a randomized comparative trial of high dose irradiation boosting with conformal protons compared with conventional dose irradiation using photons alone. Int J Radiat Oncol Biol Phys 1995;32:3–12. [PubMed: 7721636]
4. Slater JD, Rossi CJ Jr, Yonemoto LT, et al. Proton therapy for prostate cancer: the initial Loma Linda University experience. Int J Radiat Oncol Biol Phys 2004;59:348–352. [PubMed: 15145147]
5. Zietman AL, DeSilvio ML, Slater JD, et al. Comparison of conventional-dose vs high-dose conformal radiation therapy in clinically localized adenocarcinoma of the prostate: a randomized controlled trial. JAMA 2005;294:1233–1239. [PubMed: 16160131]
6. Burman C, Chui CS, Kutcher G, et al. Planning, delivery, and quality assurance of intensity-modulated radiotherapy using dynamic multileaf collimator: a strategy for large-scale implementation for the treatment of carcinoma of the prostate. Int J Radiat Oncol Biol Phys 1997;39:863–873. [PubMed: 9369136]
7. De Meerleer GO, Vakaet LA, De Gersem WR, et al. Radiotherapy of prostate cancer with or without intensity modulated beams: a planning comparison. Int J Radiat Oncol Biol Phys 2000;47:639–648. [PubMed: 10837946]
8. Ma L, Yu CX, Earl M, et al. Optimized intensity-modulated arc therapy for prostate cancer treatment. Int J Cancer 2001;96:379–384. [PubMed: 11745509]
9. Zhu S, Mizowaki T, Nagata Y, et al. Comparison of three radiotherapy treatment planning protocols of definitive external-beam radiation for localized prostate cancer. Int J Clin Onco 2005;10:398–404.
10. Zelefsky MJ, Fuks Z, Wolfe T, et al. Locally advanced prostatic cancer: long-term toxicity outcome after three-dimensional conformal radiation therapy--a dose-escalation study. Radiology 1998;209:169–174. [PubMed: 9769828]
11. Teh BS, Mai WY, Uhl BM, et al. Intensity-modulated radiation therapy (IMRT) for prostate cancer with the use of a rectal balloon for prostate immobilization: acute toxicity and dose-volume analysis. Int J Radiat Oncol Biol Phys 2001;49:705–712. [PubMed: 11172952]
12. Cella L, Lomax A, Miralbell R. Potential role of intensity modulated proton beams in prostate cancer radiotherapy. Int J Radiat Oncol Biol Phys 2001;49:217–223. [PubMed: 11163518]
13. Mock U, Bogner J, Georg D, et al. Comparative treatment planning on localized prostate carcinoma conformal photon- versus proton-based radiotherapy. Strahlenther Onkol 2005;181:448–455. [PubMed: 15995838]
14. Lomax AJ, Boehringer T, Coray A, et al. Intensity modulated proton therapy: a clinical example. Med Phys 2001;28:317–324. [PubMed: 11318312]
15. Lomax AJ, Pedroni E, Rutz H, Goitein G. The clinical potential of intensity modulated proton therapy. Z Med Phys 2004;14:147–152. [PubMed: 15462415]

NIH-PA Author Manuscript

NIH-PA Author Manuscript

NIH-PA Author Manuscript

16. Weber DC, Lomax AJ, Rutz HP, et al. Spot-scanning proton radiation therapy for recurrent, residual or untreated intracranial meningiomas. Radiother Oncol 2004;71:251–258. [PubMed: 15172139]
17. Weber DC, Trofimov AV, Delaney TF, Bortfeld T. A treatment planning comparison of intensity modulated photon and proton therapy for paraspinal sarcomas. Int J Radiat Oncol Biol Phys 2004;58:1596–1606. [PubMed: 15050341]
18. Weber DC, Rutz HP, Pedroni ES, et al. Results of spot-scanning proton radiation therapy for chordoma and chondrosarcoma of the skull base: the Paul Scherrer Institut experience. Int J Radiat Oncol Biol Phys 2005;63:401–409. [PubMed: 16168833]
19. Urie M, Goitein M, Holley WR, Chen GT. Degradation of the Bragg peak due to inhomogeneities. Phys Med Biol 1986;31:1–15. [PubMed: 3952143]
20. Bos LJ, van der Geer J, van Herk M, et al. The sensitivity of dose distributions for organ motion and set-up uncertainties in prostate IMRT. Radiother Oncol 2005;76:18–26. [PubMed: 16024120]
21. Oelfke U, Bortfeld T. Inverse planning for photon and proton beams. Med dosimetry 2001;26:113–124.
22. Trofimov A, Bortfeld T. Optimization of beam parameters and treatment planning for intensity modulated proton therapy. Technol Cancer Res Treat 2003;2:437–444. [PubMed: 14529308]
23. Nill S, Bortfeld T, Oelfke U. Inverse planning of intensity modulated proton therapy. Z Med Phys 2004;14:35–40. [PubMed: 15104008]
24. Parodi K, Poenisch F, Enghardt W. Experimental Study on the Feasibility of In-Beam PET for Accurate Monitoring of Proton Therapy. IEEE Transactions in Nuclear Science 2005:1–9.
25. Parodi K, Bortfeld T. A filtering approach based on Gaussian-powerlaw convolutions for local PET verification of proton radiotherapy. Phys Med Biol 2006;51:1991–2009. [PubMed: 16585841]
26. Engelsman M, Rosenthal SJ, Michaud SL, et al. Intra- and interfractional patient motion for a variety of immobilization devices. Med Phys 2005;32:3468–3474. [PubMed: 16372417]
27. Niemierko A. Reporting and analyzing dose distributions: a concept of Equivalent Uniform Dose (EUD). Med Phys 1997;24:17–26. [PubMed: 9029538]
28. Niemierko A. A generalized concept of equivalent uniform dose [Abstract]. Med Phys 1999;26:1100.
29. Boersma LJ, van den Brink M, Bruce AM, et al. Estimation of the incidence of late bladder and rectum complications after high-dose (70–78 GY) conformal radiotherapy for prostate cancer, using dose-volume histograms. Int J Radiat Oncol Biol Phys 1998;41:83–92. [PubMed: 9588921]
30. Wachter S, Gerstner N, Goldner G, et al. Endoscopic scoring of late rectal mucosa damage after conformal radiotherapy for prostatic carcinoma. Radiother Oncol 2000;54:11–19. [PubMed: 10719695]
31. Wachter S, Gerstner N, Goldner G, et al. Rectal sequelae after conformal radiotherapy of prostate cancer: dose-volume histograms as predictive factors. Radiother Oncol 2001;59:65–70. [PubMed: 11295208]
32. Storey JD, Pollack A, Zagars G, et al. Complications from radiotherapy dose escalation in prostate cancer: preliminary results of a randomized trial. Int J Radiat Oncol Biol Phys 2005;48:635–642. [PubMed: 11020558]
33. Benk VA, Adams JA, Shipley WU, et al. Late rectal bleeding following combined X-ray and proton high dose irradiation for patients with stages T3–T4 prostate carcinoma. Int J Radiat Oncol Biol Phys 1993;26:551–557. [PubMed: 8514551]
34. Hartford AC, Niemierko A, Adams JA, et al. Conformal irradiation of the prostate: estimating long-term rectal bleeding risk using dose-volume histograms. Int J Radiat Oncol Biol Phys 1996;36:721–730. [PubMed: 8948358]
35. Hall EJ, Wuu CS. Radiation-induced second cancers: the impact of 3D-CRT and IMRT. Int J Radiat Oncol Biol Phys 2003;56:83–88. [PubMed: 12694826]
36. Baxter NN, Tepper JE, Durham SB, et al. Increased risk of rectal cancer after prostate radiation: A population-based study. Gastroenterology 2005;128:819–824. [PubMed: 15825064]
37. Shah SK, Lui PD, Baldwin DD, Ruckle HC. Urothelial carcinoma after external beam radiation therapy for prostate cancer. J Urol 2006;175:2063–2066. [PubMed: 16697804]
38. Hall EJ. Intensity-modulated radiation therapy, protons, and the risk of second cancers. Int J Radiat Oncol Biol Phys 2006;65:1–7. [PubMed: 16618572]

NIH-PA Author Manuscript

NIH-PA Author Manuscript

NIH-PA Author Manuscript

39. Paganetti H, Bortfeld T, DeLaney TF. Neutron dose in scattered and scanned proton beams. Int J Radiat Oncol Biol Phys 2006;66:1594–1595. [PubMed: 17126219]

40. Schneider U, Lomax A, Pemler P, et al. The impact of IMRT and proton radiotherapy on secondary cancer incidence. Strahlenther Onkol 2006;182:647–652. [PubMed: 17072522]

NIH-PA Author Manuscript

NIH-PA Author Manuscript

NIH-PA Author Manuscript

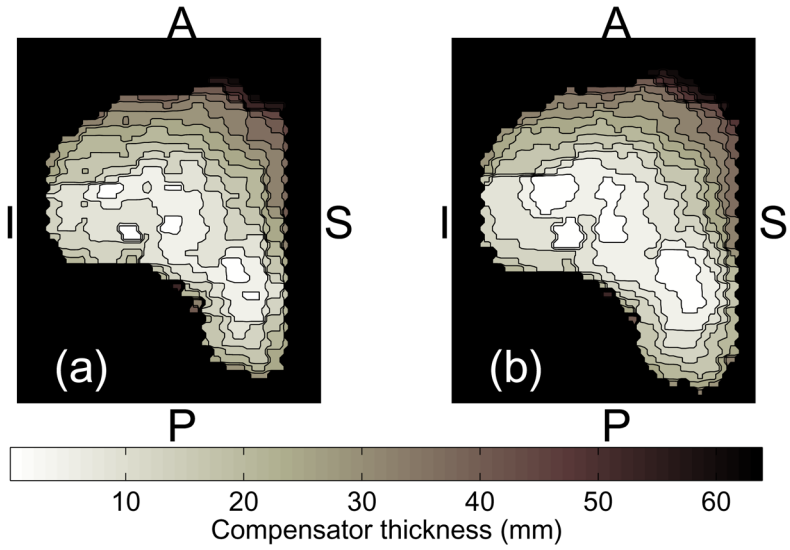

Figure 1.
A proton range compensator map: (a) designed based on the radiological depth of the target's distal edge; and (b) smeared to counter the range uncertainties. The letters indicate anterior (A), posterior (P), inferior (I) and superior (S) directions.

NIH-PA Author Manuscript

NIH-PA Author Manuscript

NIH-PA Author Manuscript

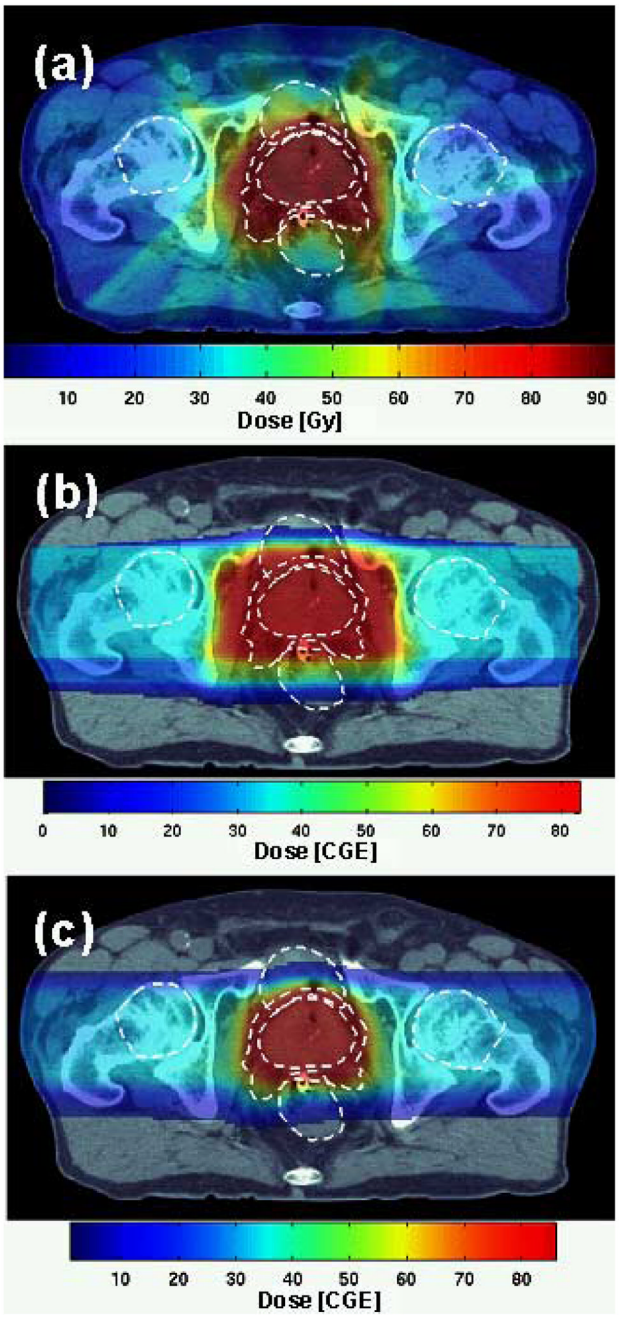

Figure 2.
Patient 1: dose distribution in the transversal isocenter section from (a) IMRT, (b) 3D-CPT and (c) IMPT plans. Dashed white lines show the contours of the prostate, PTV1, rectum, bladder and femoral heads.

NIH-PA Author Manuscript

NIH-PA Author Manuscript

NIH-PA Author Manuscript

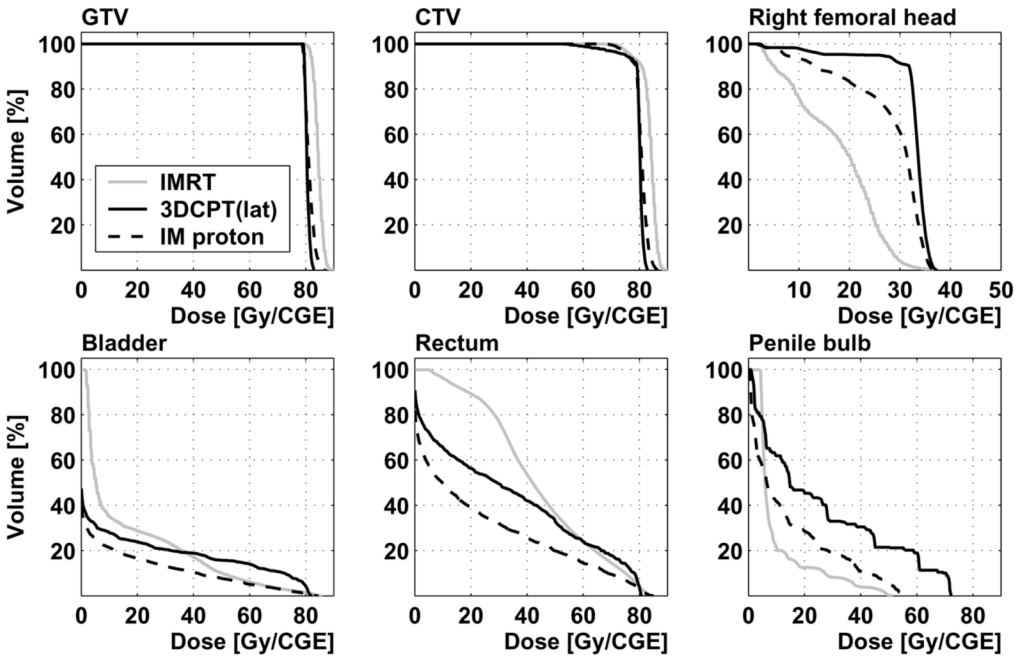

Figure 3.
Patient 1: dose-volume histograms from IMRT, 3D-CPT (parallel-opposed lateral beam configuration, labeled “lat”) and IMPT plans

NIH-PA Author Manuscript

NIH-PA Author Manuscript

NIH-PA Author Manuscript

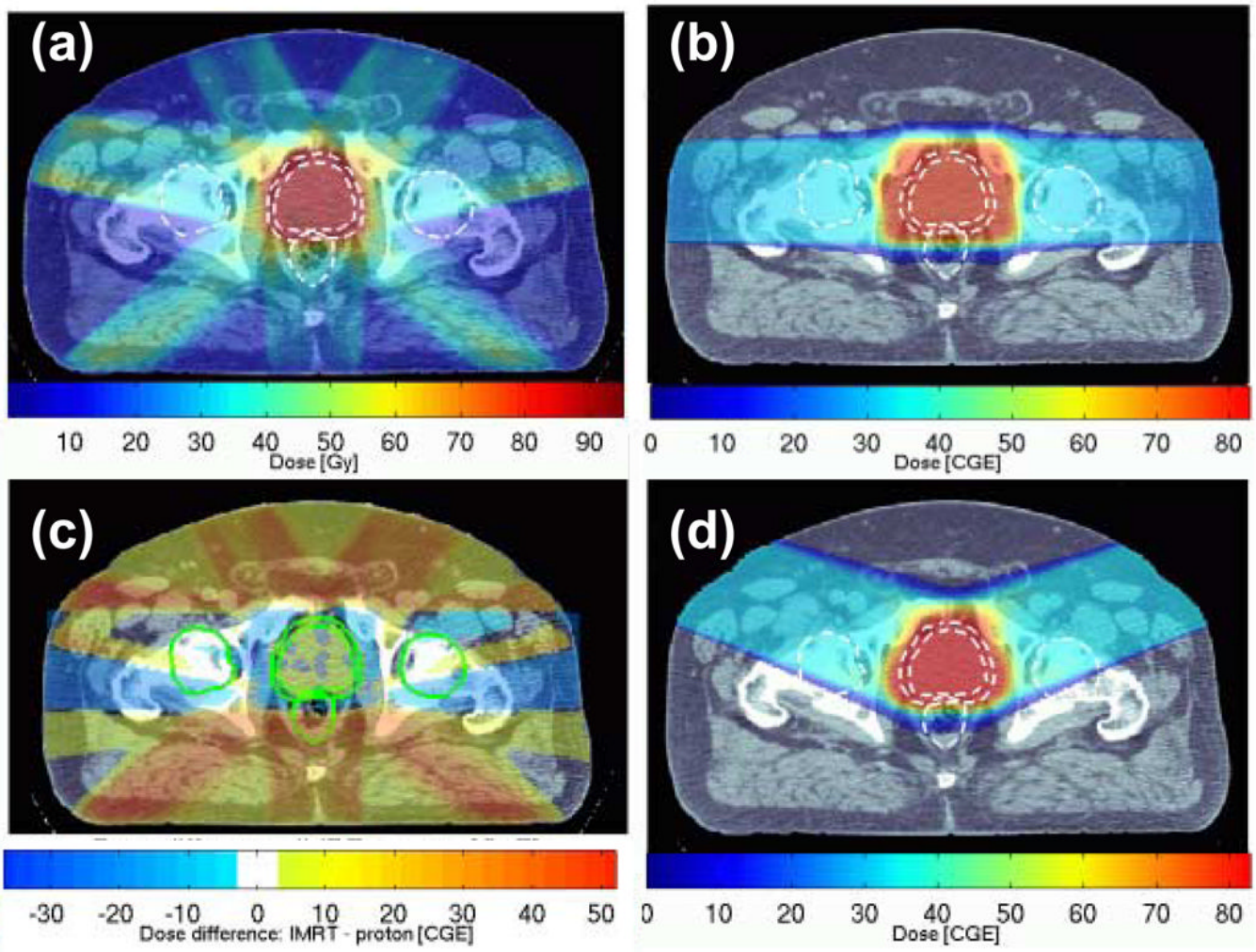

Figure 4.

Patient 2: dose distributions from (a) IMRT, (b) 3D-CPT plan using parallel-opposed lateral beam configuration; the difference between doses delivered by these two plans is shown in (c). Dose distribution from the 3D-CPT plan using lateral-anterior-oblique beam configuration, with the beams rotated by 20° towards the anterior, is shown in (d). The outlines of the prostate, PTV1, rectum and femoral heads are designated as dashed white lines in (a, b, d), and solid green lines in (c).

NIH-PA Author Manuscript

NIH-PA Author Manuscript

NIH-PA Author Manuscript

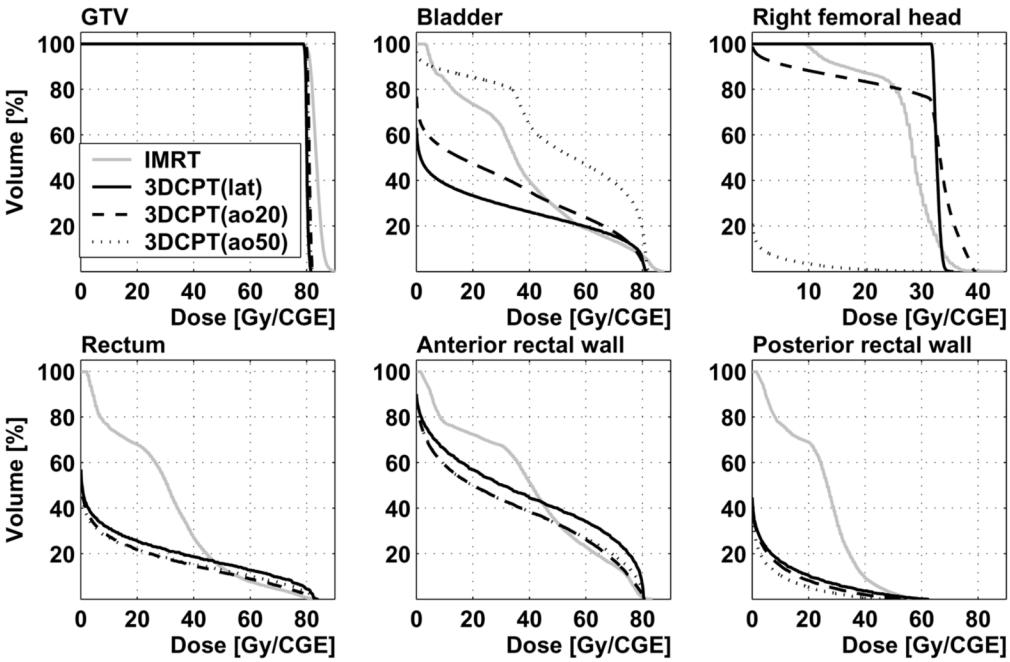

Figure 5.

Patient 2: dose-volume histograms from IMRT and 3D-CPT plans with lateral parallel-opposed ("lat"), and anterior-oblique configurations with the beams rotated by 20° ("ao20") and 50° ("ao50") towards the anterior. DVH are shown for the gross tumor volume, bladder, right femoral head, whole rectum, anterior and posterior rectal walls.

NIH-PA Author Manuscript

NIH-PA Author Manuscript

NIH-PA Author Manuscript

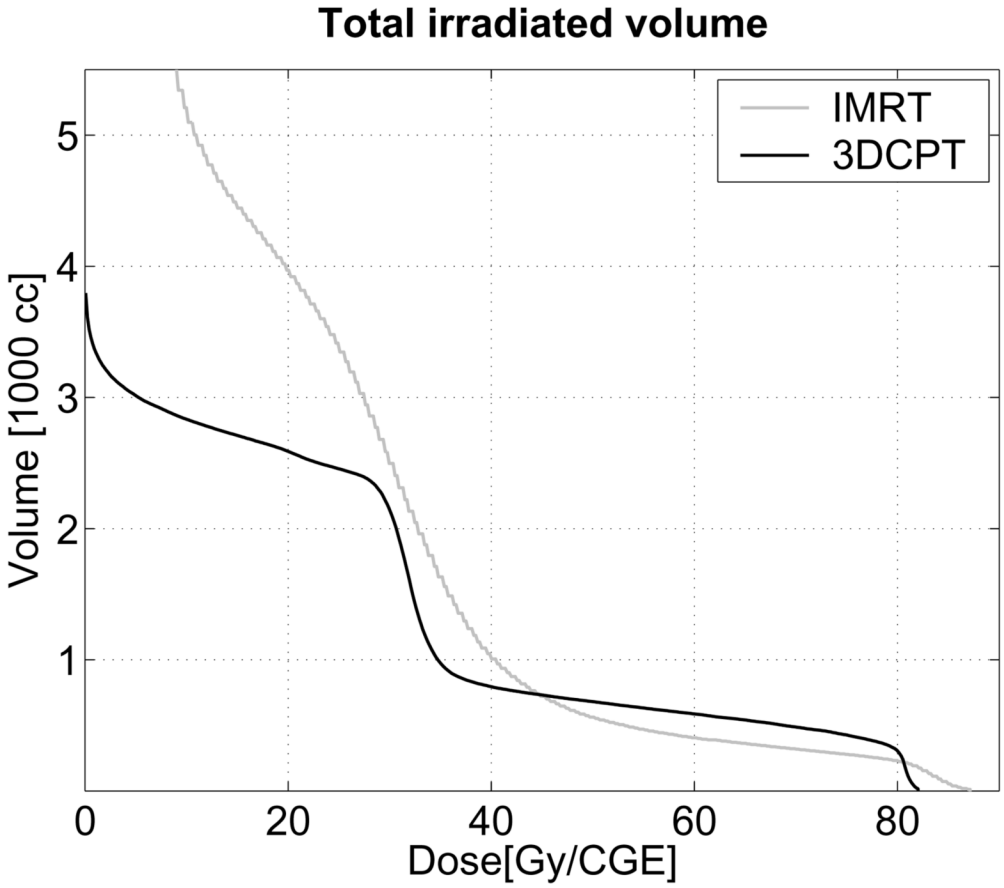

Figure 6.
Patient 2: dose-volume histograms for the whole irradiated body volume.

NIH-PA Author Manuscript

NIH-PA Author Manuscript

NIH-PA Author Manuscript

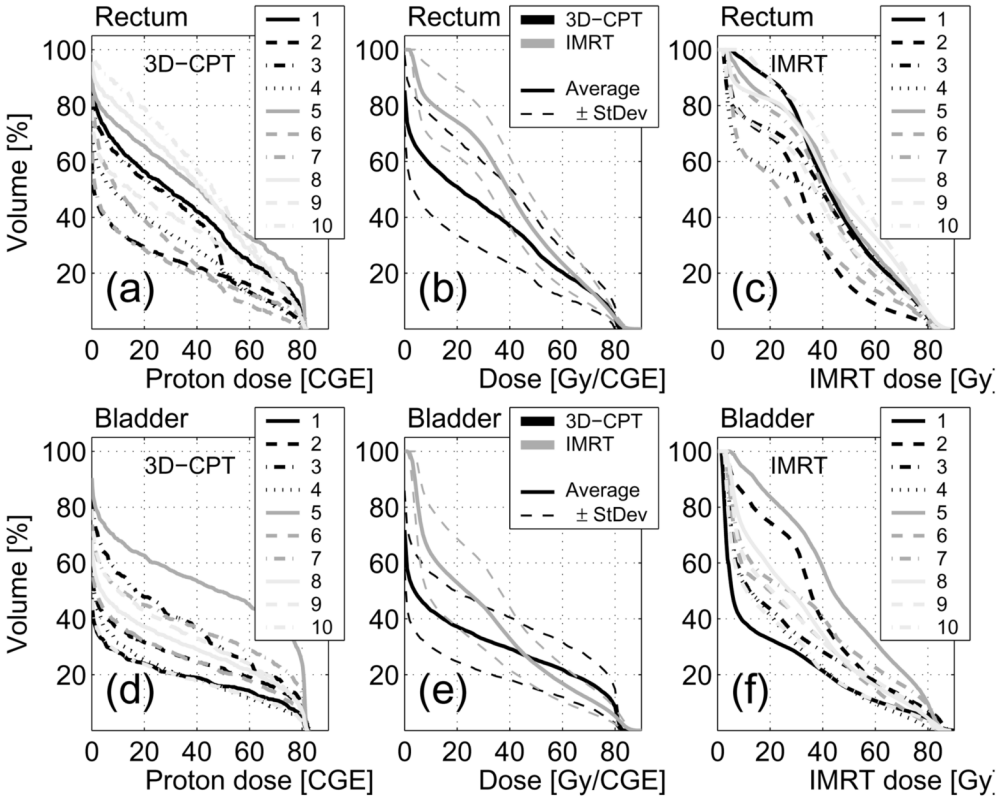

Figure 7.

Dose-volume histograms for the rectum (a-c) and bladder (d-f). Individual DVH from ten 3D-CPT and IMRT plans are shown in (a, d) and (c, f), respectively. Plots (b) and (e) show curves obtained by averaging, over the irradiated volume, of the DVH from 10 plans, as well as one-standard-deviation variability bounds (dashed lines).

NIH-PA Author Manuscript
NIH-PA Author Manuscript
NIH-PA Author Manuscript

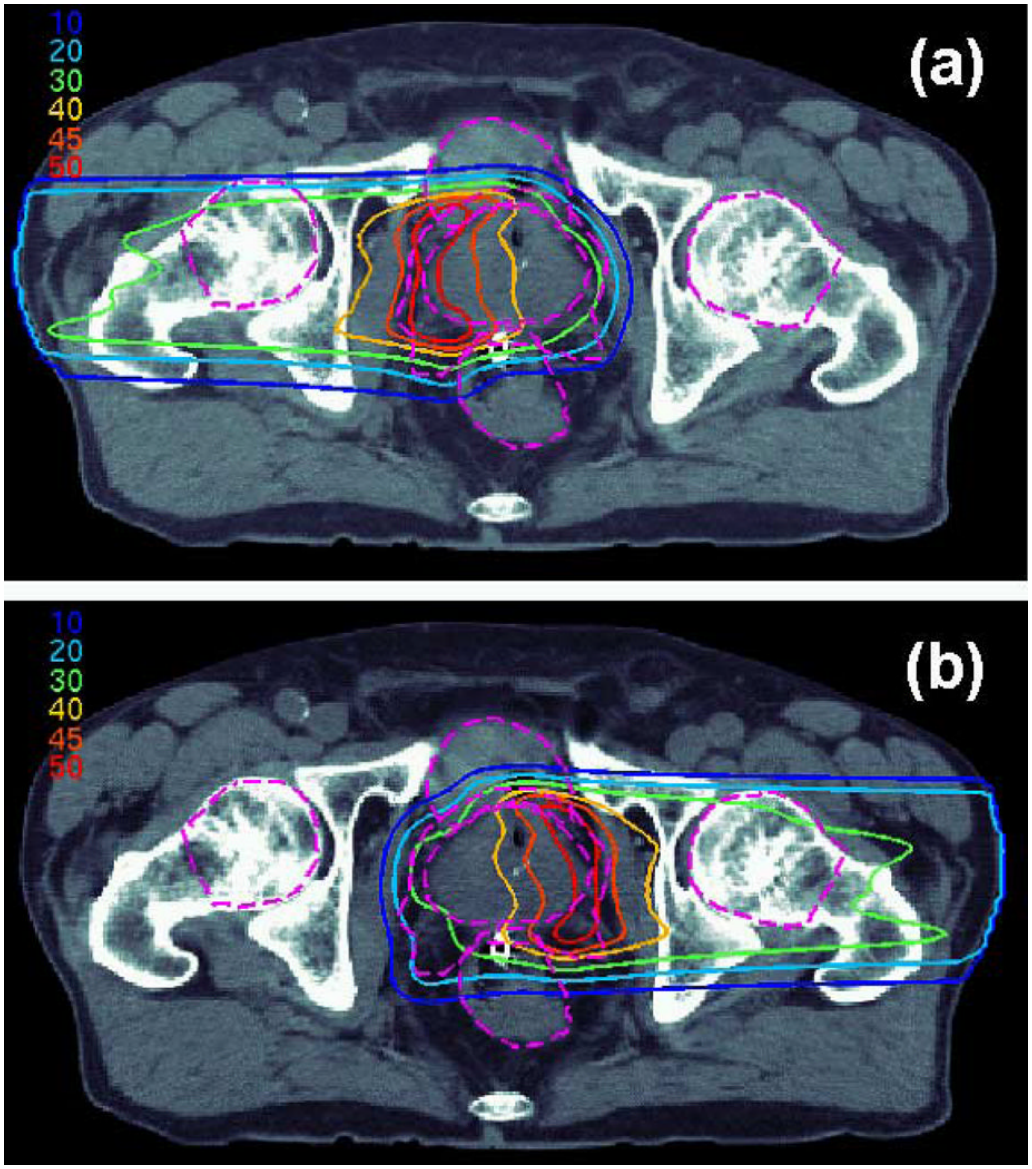

Figure 8.
Patient 1: IMPT dose distributions delivered by (a) the right lateral and (b) left lateral beams. Dashed purple lines designate the outlines of the prostate, PTV1, rectum, bladder and femoral heads.

NIH-PA Author Manuscript

NIH-PA Author Manuscript

NIH-PA Author Manuscript

Table 1

Treatment plan objectives

Target prescription doses	
GTV (Prostate)	100% to 79.2 Gy/CGE
CTV (GTV & seminal vesicles)	100% to 50.4 Gy/CGE
PTV2 (GTV + 5 mm margin)	98% to 79.2 Gy/CGE
PTV1 (CTV + 5 mm margin)	98% to 50.4 Gy/CGE
Tolerance doses for healthy organs	
Rectum	<50% to 60 Gy/CGE <35% to 65 Gy/CGE <25% to 70 Gy/CGE <15% to 75 Gy/CGE maximum 84.7 Gy/CGE
Bladder	<50% to 65 Gy/CGE <35% to 70 Gy/CGE <25% to 75 Gy/CGE <15% to 80 Gy/CGE maximum 84.7 Gy/CGE
Femoral Head	maximum 50 Gy/CGE
Penile Bulb	mean dose < 52.5 Gy/CGE

Abbreviations: GTV = gross tumor volume; CGE = cobalt Gray-equivalent; CTV = clinical target volume; PTV = planning target volume.

NIH-PA Author Manuscript NIH-PA Author Manuscript NIH-PA Author Manuscript

Table 2

Size of target volumes, total volume of tissue irradiated to prescription doses, and conformity indices for PTV1.

	Target volume (cc)			Volume irradiated to 79.2 Gy/CGE (cc)		Volume irradiated to 50.4 Gy/CGE (cc)		PTV1 conformity index	
Case	GTV	PTV2	PTV1	IMRT	3D-CPT	IMRT	3D-CPT	IMRT	3D-CPT
1	54	104	145	138	185	374	442	2.58	3.05
2	116	194	223	240	348	562	686	2.52	3.08
3	30	68	96	96	130	278	322	2.90	3.35
4	49	99	122	113	179	363	400	2.98	3.28
5	120	205	249	264	360	681	721	2.73	2.90
6	55	107	150	138	173	403	398	2.69	2.65
7	85	156	179	206	246	512	540	2.86	3.02
8	56	112	142	136	192	365	443	2.57	3.12
9	56	113	138	138	181	378	447	2.74	3.23
10	49	96	114	116	169	317	387	2.78	3.39
Mean	67	125	156	159	216	423	479	2.73	3.11

Abbreviations: CGE = cobalt Gray-equivalent; GTV = gross tumor volume; PTV = planning target volume; IMRT = intensity-modulated radiotherapy; 3D-CPT = 3D-conformal proton therapy.

NIH-PA Author Manuscript NIH-PA Author Manuscript NIH-PA Author Manuscript

Table 3

Minimum, mean and maximum doses planned for target volumes.

Target volume	Dose metric	IMRT plans [Gy]		3D-CPT plans [CGE]	
		Average of 10 plans	Range (min - max)	Average of 10 plans	Range (min - max)
GTV	D-min	79.9	79.2 – 82.3	79.5	79.2 – 80.3
	D-mean	83.5	81.7 – 86.1	81.1	80.4 – 82.4
	D-max	87.7	84.3 – 90.0	83.2	82.0 – 85.4
CTV	D-min	69.4	62.0–74.9	60.8	52.2 – 75.2
	D-mean	83.0	81.0 – 84.5	80.4	77.6 – 81.8
	D-max	87.7	84.3 – 90.0	83.2	82.0 – 85.4

Abbreviations: CGE = cobalt Gray-equivalent; GTV = gross tumor volume; CTV = clinical target volume; IMRT = intensity-modulated radiotherapy; 3D-CPT = 3D-conformal proton therapy; D-min = minimum dose; D-mean = mean dose; D-max = maximum dose.

NIH-PA Author Manuscript NIH-PA Author Manuscript NIH-PA Author Manuscript

Table 4

Dose-volume metrics of IMRT and proton plans, for the rectum and bladder. The *p*-values of the Wilcoxon matched-pair signed-rank test reflect the significance of the difference between respective metrics of 10 sets of IMRT and 3D-CPT plans, with the statistically significant level set at $p \leq 0.05$.

Volume	Metric	IMRT plans		3D-CPT plans		
		Average	Range (min - max)	Average	Range (min - max)	*p* - value
Rectum	D-mean [Gy/CGE]	39.4	28.5 – 50.9	29.2	17.2 – 43.7	0.002
	$D_{35\%}$ [Gy/CGE]	49.4	35.2 – 62.0	37.5	9.8 – 57.2	0.010
	$D_{25\%}$ [Gy/CGE]	57.4	42.7 – 69.0	50.6	27.8 – 72.7	0.084
	$D_{15\%}$ [Gy/CGE]	67.3	50.8 – 75.5	65.1	49.2 – 79.9	0.492
	$D_{2\%}$ [Gy/CGE]	81.6	79.1 – 83.6	80.2	77.3 – 81.3	0.055
	V_{30} [%]	65.3	41.2 – 81.6	43.8	23.5 – 68.2	0.002
	V_{50} [%]	34.4	15.8 – 53.2	28.2	14.2 – 44.9	0.027
	V_{60} [%]	23.6	9.0 – 38.0	20.4	8.6 – 33.0	0.232
	V_{70} [%]	14.5	5.2 – 23.5	14.0	4.9 – 26.5	0.770
	V_{75} [%]	9.7	3.6 – 15.9	10.3	2.8 – 21.3	0.922
Bladder	D-mean [Gy/CGE]	29.9	19.9 – 46.3	24.1	14.8 – 43.2	0.006
	$D_{35\%}$ [Gy/CGE]	35.6	15.2 – 56.9	26.0	2.2 – 74.6	0.084
	$D_{25\%}$ [Gy/CGE]	47.3	34.6 – 66.3	44.6	15.9 – 79.9	0.432
	$D_{15\%}$ [Gy/CGE]	61.5	50.0 – 76.5	67.4	49.2 – 80.9	0.006
	$D_{2\%}$ [Gy/CGE]	82.7	78.0 – 85.8	81.6	80.9 – 82.1	0.160
	V_{30} [%]	44.5	28.0 – 74.3	32.8	20.6 – 57.4	0.006
	V_{50} [%]	23.7	15.0 – 42.2	25.4	14.6 – 49.6	0.193
	V_{60} [%]	16.9	9.7 – 31.8	21.9	11.5 – 45.1	0.002
	V_{70} [%]	11.4	5.7 – 21.5	17.3	8.3 – 39.0	0.002

Abbreviations: IMRT = intensity-modulated radiotherapy; 3D-CPT = 3D-conformal proton therapy; D-mean = mean dose; CGE = cobalt Gray-equivalent; $D_n\%$ = dose received by *n*% of the organ volume; V_n = share of the organ volume that received at least *n* Gy/CGE.

NIH-PA Author Manuscript NIH-PA Author Manuscript NIH-PA Author Manuscript

Table 5

The values of the equivalent uniform dose (EUD), with margins of uncertainty, for the gross tumor volume, whole rectal volume and bladder.

Volume	EUD exponent (α)	IMRT EUD [Gy]		3D-CPT EUD [CGE]	
		Average of 10 plans	Range (min - max)	Average of 10 plans	Range (min - max)
GTV	-10^{+3}_{-5}	83.4 (±0.04)	81.7 – 86.1	81.1 (±0.02)	80.3–82.4
Rectum	5^{+3}_{-2}	$56.4^{+5.6}_{-6.1}$	$48.3^{+7.4}_{-6.9} - 62.2^{+4.0}_{-4.3}$	$54.8^{+6.4}_{-7.9}$	$46.4^{+7.8}_{-8.7} - 62.3^{+5.1}_{-6.6}$
Bladder	7^{+5}_{-3}	$59.0^{+7.4}_{-8.9}$	$53.0^{+8.0}_{-9.5} - 65.0^{+5.3}_{-6.2}$	$61.4^{+6.6}_{-9.1}$	$56.4^{+8.2}_{-10.9} - 70.0^{+3.8}_{-5.5}$

Abbreviations: EUD = equivalent uniform dose; IMRT = intensity-modulated radiotherapy; 3D-CPT = 3D-conformal proton therapy; CGE = cobalt Gray-equivalent; GTV = gross tumor volume.